Final Summary Report

Plant cell walls are complex and highly dynamic structures, changing composition and structure during growth and development and in response to biotic and abiotic stresses. In parallel, dwindling supplies of fossil fuels and growing energy demands make plant cell walls more and more important for bioenergy production. As the amount of energy produced from lingo-cellulosic biomass is dependent on quantity and quality of biomass, an understanding of the mechanisms and signalling pathways involved in coordinating cell wall composition and remodelling is crucial for improving efficiency of energy production from renewable biomass resources. The aim of this project was to understand the role of hexoses in the response of the cell wall to stress/damage and to characterise the regulatory mechanism that coordinates cellulose biosynthesis with photosynthetic activity and carbohydrate metabolism. In this study, the pre-emergence herbicide isoxaben was used to cause cell wall damage through cellulose biosynthesis inhibition (CBI) in *Arabidopsis* seedlings grown in liquid culture and the response was studied using FRET-based nanosensors, RT-PCR based expression analysis and phenotypic characterization.

To investigate the function of sugar/hexoses in the response to CBI, we applied a FRET-based nanosensor technique to monitor the effect of isoxaben on cellular sugar distribution. From our collaboration partners (Frommer Group at the Carnegie Department of Plant Biology, Stanford, USA) I obtained seeds of five different nanosensor expressing plant lines and the necessary knowledge and expertise to visualise glucose and sucrose in living plant cells. The four glucose and single sucrose sensors have different affinities (3.2mM, 600µM, 2µM, 170nM and 90µM) and are located in the cytosol. Sugar contents were monitored for up to one hour (after start of treatment) in epidermal cells of the root elongation zone of 5 day old seedlings (Fig 1). In every measurement the sensor activity was first tested by infusing the seedling with sugar solutions of different concentrations, which caused a decrease in the FRET (CFP/YFP) ratio. After the nanosensor had returned to its initial state the seedling was infused with media containing a moderate sugar concentration and 600nM isoxaben. However, no change in FRET ratio was observed in any of the measurements with the different nanosensors, suggesting that isoxaben treatment does not cause changes in cytosolic sugar concentrations in the epidermis of the plants analysed. The next step was to cross the nanosensor expressing plants with *Arabidopsis* mutants that are affected in cellular sugar distribution (*tonoplast monosaccharide transporter1-2-3, tmt1-2-3*), JA signalling (*jasmonic acid resistant1, jar1*) and sensing of plasmamembrane tension (*mechanosensitive channel of small conductance-like, msl*), to analyse the effects of the mutations on the intracellular sugar contents. In addition, our collaboration partners generated plant lines expressing nanosensors targeted to the apoplast and constructs for expression in the vacuole. The apoplastic lines were crossed with different *Arabidopsis* mutants to monitor the effects of the mutation on extracellular sugar contents in comparison to wildtype. The cell wall mutants selected for this analysis were the arabinose-mutant *murus4* (*mur4*) previously implicated in hexose signalling, the photomorphogenesis mutant *de-etiolated1* (*det1*) and the vacuolar H(+)-ATPase mutant *de-etiolated3* (*det3*). All the crosses are now in the F2 generation and selection of homozygous lines is under way. The vacuolar constructs were transformed into *Arabidopsis* but did not result in sufficient fluorescence, probably due to the acidity of the vacuole that probably affects the stability of the fluorescent proteins negatively. In conclusion, isoxaben seems not to cause changes in cytoplasmic sugar contents, possibly due to a redistribution of sugars into the vacuole or because extracellular sugar levels are affected during CBI. However, due to the limited time available, the alternative possibilities could not be pursued further.

Hamann et al. 2009 found that lignin deposition caused by isoxaben was dependent on hexose availability, suggesting a role of hexose in signalling. Cell wall invertases can function as initial detectors for sensing of extracellular sugars, by splitting sucrose into glucose and fructose. Microarray data of a time course showed transcriptional activation of two cell wall invertase encoding genes (*ATCWINV1* and *6*) in response to isoxaben treatment. To analyse the role of ATCWINV1 and 6 during the response to CBI, expression levels of both genes were determined by semi-quantitative RT-PCR (Fig 2a). T-DNA insertion lines for the two genes were obtained from the stock centre and plants homozygous for the insertions were identified (Fig 2b). RT-PCR analysis for *ATCWINV6* showed that the insertion in SK_136281 resulted in a loss of gene expression, whereas in SK_152299 a transcript was detectable. In none of the three insertion lines for *ATCWINV1* a transcript was detectable (Fig 2c). A general growth analysis was performed and did not show any significant differences in early growth stages. However, all three *cwinv1* mutants showed an early flower phenotype, whereas the *cwinv6* mutant displayed a flowering time

similar to wildtype (Fig 2d). To investigate the role of invertases in the response to CBI, lignin staining was performed 12h and 24h after isoxaben treatment. After 12h, *cwinv6* showed significantly less lignin deposition in the root elongation zone compared to wildtype, which was less pronounced after 24h. By contrast, seedlings from all three *cwinv1* lines exhibited staining patterns similar to wildtype after 12h and 24h of CBI (Fig 2e). Measurements of soluble sugar and starch contents in response to CBI showed that the *ATCWINV1* mutants contained significantly lower levels of glucose and fructose after 10h of mock treatment (data not shown). However, these sugar levels were further reduced during isoxaben treatment, suggesting an intact cell wall damage response. The cwinv6 mutant showed a similar response to CBI compared to wildtype (Fig 2f). To confirm that the lignin phenotype of *atcwinv6* is caused by the knockout of the gene, I generated two inducible complementation constructs. In the first construct the *ATCWINV6* gene was fused to a HA-tag under the control of a heat-shock promoter, in the second construct the fluorescent protein citrine was used instead of the tag. Both constructs have been transformed into the *atcwinv6* mutant and selection for positive transformants is under way. For expression analysis of *ATCWINV6* a promoter-GUS construct was generated and transformed into wildtype plants. Selection using hygromycin and subsequent PCR genotyping identified 22 independent primary transformants ready to use. In conclusion, the response to CBI does not seem to be affected in *ATCWINV1* mutants, whereas the *atcwinv6* mutant seems to be involved in the isoxaben effect on lignin deposition. The transgenic lines for complementation and further detailed analysis of *ATCWINV6*, such as determination of the subcellular localisation of the protein, activity studies of the protein, expression profiling using promoter-reporter fusion, are now available.

Our preliminary data supported the idea of a regulatory mechanism coordinating cell wall with primary metabolism. I confirmed initial microarray derived-expression data that CBI leads to transcriptional shutdown of genes involved in photosynthesis, the Calvin Cycle and starch degradation by qRT-PCR (Fig 3a). Soluble sugar and starch measurements showed that glucose, fructose and sucrose decrease in isoxaben treated seedlings, whereas starch contents increase over time compared to mock treated plants (Fig 3b and c). Using the isoxaben resistant mutant *ixr1-1*, I showed that the observed effects are CBI specific (Fig. 3e). In addition, metabolic profiling experiments, performed by our collaboration partners (Dr. A. Nunez-Nesi, Dr. Alisdair Fernie, MPI Golm, Germany) showed that isoxaben treatment causes a redirection of metabolic flux away from the cell wall towards starch biosynthesis (Fig 3d). By collaborating with Dr. Laura Barter´s group at Imperial College, we showed that CBI also causes a reduction in Rubisco activity and therefore affects photosynthetic performance (Fig 3f). I showed that the observed effects on the transcriptional and metabolic level can be suppressed in a concentration dependent manner by providing osmotic support using PEG (Fig 4a and b). In parallel, hyper-osmotic stress treatments such as NaCl and KCl had opposite effects on sucrose and starch levels of the seedling (Fig 4c). These observations suggested that turgor pressure can be a regulator of the coordination of source-sink relationships. To dissect the signalling pathways mediating the CBI-induced and osmosensitive changes in primary metabolism/gene expression I screened *Arabidopsis* mutants impaired in sugar signalling, regulation of sugar distribution, osmosensing, cell wall signalling, ROS production and mechanoperception (Fig 5a). In *mid1 complementing activity* (*mca1* encoding a putative stretch activated Ca2+ channel), *Arabidopsis histidine kinase* (*ahk4*, osmosensor) and *respiratory burst oxidase homolog DF* (*rbohDF*, NADPH oxidase) seedlings the CBI induced effects on starch metabolism and gene expression were not suppressed by osmotic support (Fig 5b and c), suggesting that these genes are required for the observed osmotic effects. These findings reveal a novel regulatory mechanism coordinating cellulose biosynthesis with primary metabolism and carbon fixation in plants. We demonstrate that the osmotic state of the cell affects carbohydrate metabolism and identify *MCA1*, *AHK4* and NADPH oxidase derived ROS production as components of the signalling mechanism translating osmotic signals into metabolic changes. These results are presented in a manuscript currently under review at PNAS.

To summarise, results of this project are of interest for researchers aiming to optimize bioenergy production by increasing carbon fixation in plants. The observation that the osmotic state of a cell acts as an indicator and/or regulator for the state of the metabolism is a completely novel concept and of interest for scientists working on regulation of plant metabolism. Furthermore, the insights into the underlying molecular mechanism of turgor driven metabolic regulation open up new possibilities to manipulate plant metabolism, for example to improve crop performance.

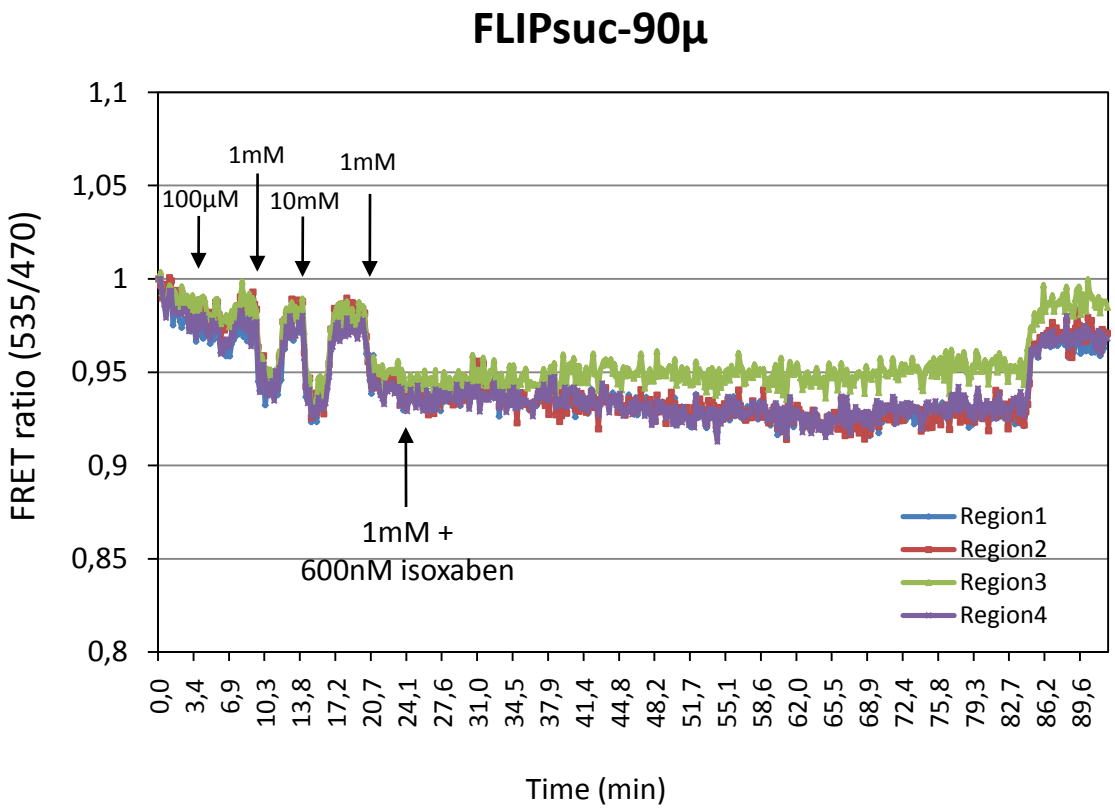

Figure 1. Monitoring of sucrose contents with the sucrose-nanosensor FLIPsuc-90µ. Measurements of the FRET ratio were taken in four different epidermal cells (region1 to 4) of the root elongation zone. The seedling was first perfused with 100µM, 1mM and 10mM sucrose solution to test the sensor activity. Effect of Isoxaben was monitored by perfusing with 1mM sucrose and 600nM isoxaben for 60 minutes.

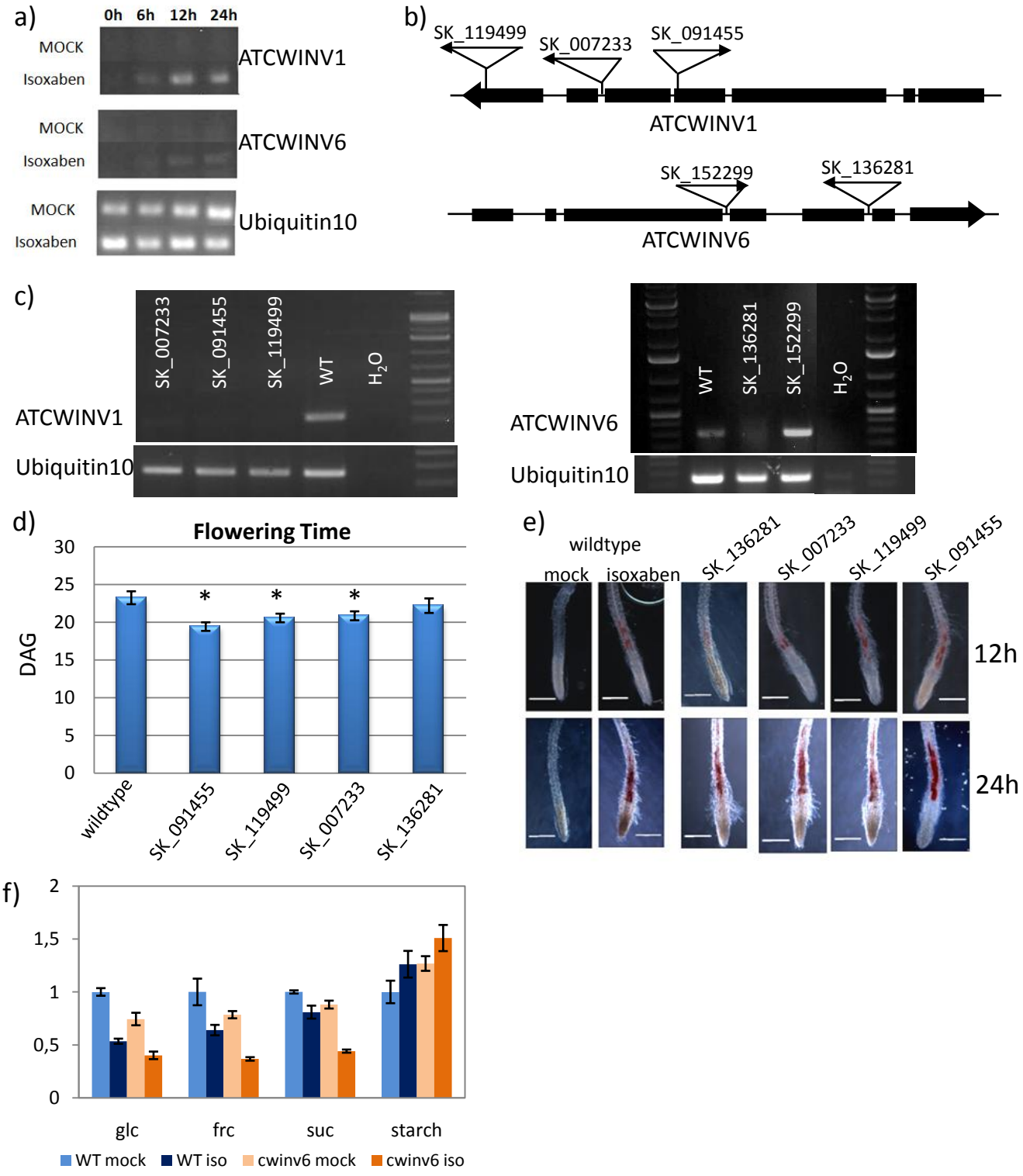

Figure2. Analysis of ATCWINV1 and 6 in the response to CBI.

a) Semi-quantitative RT-PCR of *ATCWINV1* and *6* in response to CBI. **b)** Gene models of *ATCWINV1* and *6* with insertion sites. **c)** RT-PCR of *ATCWINV1* and *6* insertion lines. Genespecific primers for *ATCWINV1, ATCWINV6* and *Ubiquitin10* (as a loading control) were used. **d)** flowering time was counted as days after germination (DAG) when the main stem was 1cm. Asterisks indicate statistically significant differences (t-test, $P < 0.05$); **e)** Lignin staining of *cwinv1* lines, *cwinv6* and wildtype after 12h and 24h of isoxaben treatment. Bars stand for 0.5mm; **f)** Soluble sugar and starch contents after 10h of mock and isoxaben treatment in wildtype (blue) and *cwinv6* mutant (orange). Columns represent the means with error bars (SD) from three biological replicates. Data was normalized to Col-0 mock-treated sample.

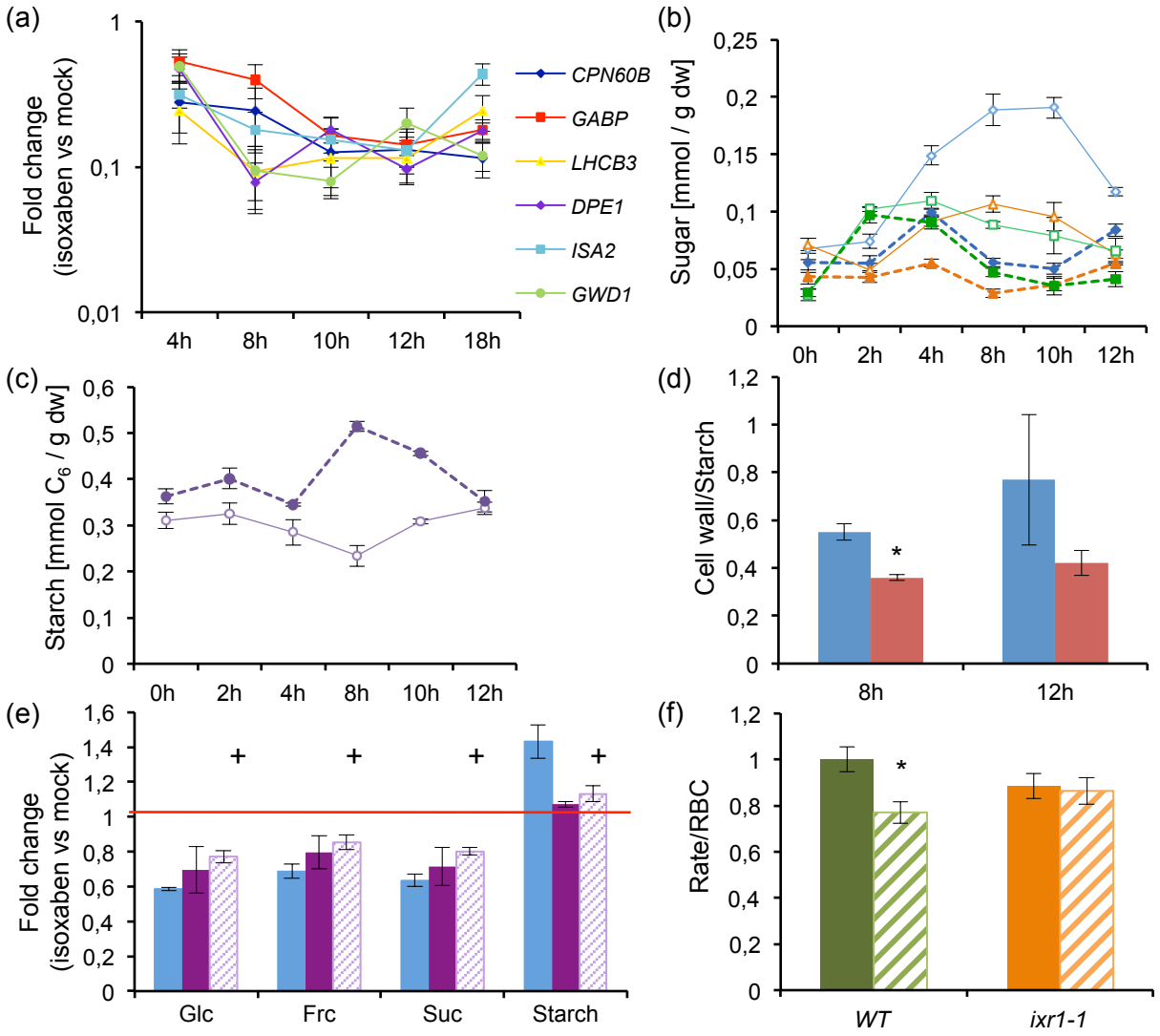

Figure 3. Effects of CBI on primary metabolism and photosynthesis.
a) qRT-PCR expression analysis of genes involved in photosynthesis and starch metabolism. Columns represent the means with error bars (SD) from three biological replicates.
b) Changes in glucose (blue), fructose (orange) and sucrose (green) contents in mock (solid line) and isoxaben (dashed line) treated seedlings over time. **c**) Changes in starch content in mock (solid line) and isoxaben (dashed line) treated seedlings over time. **d**) Metabolic flux measurement using ^{14}C-labelled sucrose. Each column represents the ratio of flux into cell wall vs flux into starch in seedlings after 8h and 12h of mock (blue) and CBI (red) treatment. Values are the means with error bars (SD) of three biological replicates. * indicates statistical significant difference t-test $p < 0.05$ **e)** Data was normalized to Col-0 mock-treated sample. Soluble sugar and starch contents of Col-0 (blue) and *ixr1-1* (purple) seedlings incubated without (dark purple) or with isoxaben (blue/light purple) for 10h. + indicate statistical significant difference compared to Col-0 isoxaben-treated samples. **f)** Specific Rubisco activity in Col-0 (green) and *ixr1-1* (orange) seedlings incubated with (light colour) or without (dark colour) isoxaben for 10h. Values are means from 6 biological replicates, each consisting of three technical replicates. Error bars based on SD (n=18). Data was normalized to the Col-0 mock-treated sample. Values in (b, c, e) are means with error bars (SD) (n≥3). Data representative for at least three independent experiments.

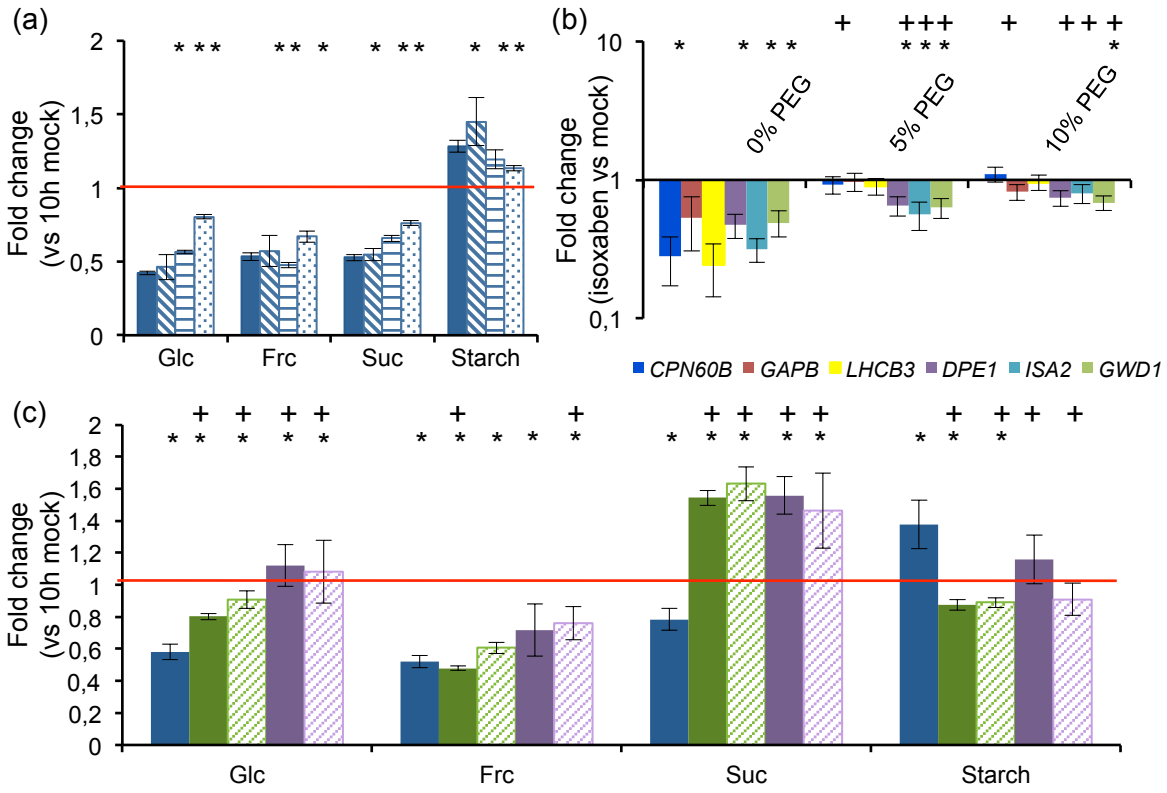

Figure 4. Effects of hypo- and hyperosmotic treatment on primary metabolism. **a**) Sugar and starch contents of Col-0 seedlings treated with isoxaben (blue), with isoxaben/ 2.5% PEG (hashed blue), with isoxaben/5%PEG (horizontal blue lines), with isoxaben/10% PEG (dotted blue) for 10h. Data was normalized to the Col-0 mock-treated sample without PEG, highlighted by red line. * indicate statistical significant difference compared to mock-treated samples. **b**) qRT-PCR expression analysis of genes involved in photosynthesis and starch metabolism after 4h of treatment with isoxaben; isoxaben/ 5%PEG and isoxaben/10%PEG. Values are means and SEM from three biological replicates. + indicate statistical significant difference compared to the expression of the same gene in isoxaben-treated samples. * indicate statistical significant difference compared to the expression of the same gene in mock-treated samples. **c**) Sugar and starch contents of Col-0 seedlings treated with isoxaben (blue), 100mM KCl (green), 150mM KCl (shaded green), 100mM NaCl (purple), 150mM NaCl (hashed purple). + indicate statistical significant difference compared to isoxaben-treated samples. * indicate statistical significant difference compared to mock-treated samples. Data were normalized to Col-0 mock-treated sample.Values in (a, c) are the means with error bars (SD) of three replicates (n≥3). Data representative for three independent experiments.

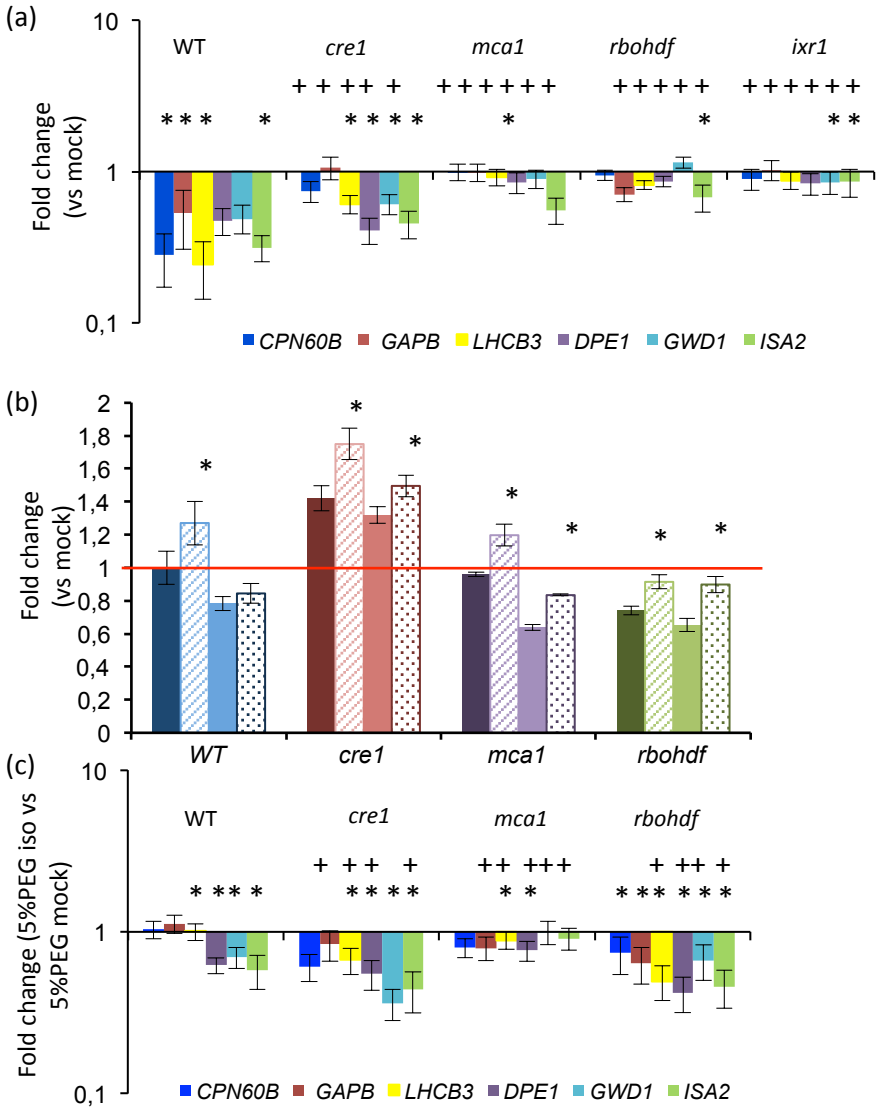

Figure 5. Functional analysis of genes potentially involved in the CWD response and osmo-sensing.

a) qRT-PCR expression analysis of genes involved in photosynthesis and starch metabolism after 4h of isoxaben treatment in Col-0 and mutants. Values are the means with error bars (SEM) from three biological replicates. + indicate statistical significant difference compared to the expression of the same gene in isoxaben-treated Col-0 samples. * indicate statistical significant difference compared to the expression of the same gene in mock-treated samples.**b**) Starch contents of Col-0 (blue), *ahk4* (red), *mca1* (purple) and *rbohdf* (green) seedlings incubated with isoxaben (shaded), without isoxaben (solid), without 5%PEG (light) or with isoxaben/5% PEG (dotted) for 10h. Data was normalized to the Col-0 mock-treated sample without PEG. Values are the means with error bars (SD) from three biological replicates (n≥3). Data representative for at least three independent experiments. * indicate statistical significant difference compared to mock-treated samples. **c**) qRT-PCR of genes involved in photosynthesis and starch metabolism after 4h of combined treatment with isoxaben/5% PEG in Col-0 and mutants. Values are the means with error bars (SEM) from three biological replicates. + indicate statistical significant difference compared to the expression of the same gene in isoxaben-treated Col-0 samples. * indicate statistical significant difference compared to the expression of the same gene in mock-treated samples.